



OPEN

Dynamics of chaotic system based on circuit design with Ulam stability through fractal-fractional derivative with power law kernel

Naveed Khan¹, Zubair Ahmad², Jamal Shah¹, Saqib Murtaza³, M. Daher Albalwi⁴, Hijaz Ahmad^{5,6}, Jamel Baili^{7,8} & Shao-Wen Yao⁹✉

In this paper, the newly developed Fractal-Fractional derivative with power law kernel is used to analyse the dynamics of chaotic system based on a circuit design. The problem is modelled in terms of classical order nonlinear, coupled ordinary differential equations which is then generalized through Fractal-Fractional derivative with power law kernel. Furthermore, several theoretical analyses such as model equilibria, existence, uniqueness, and Ulam stability of the system have been calculated. The highly non-linear fractal-fractional order system is then analyzed through a numerical technique using the MATLAB software. The graphical solutions are portrayed in two dimensional graphs and three dimensional phase portraits and explained in detail in the discussion section while some concluding remarks have been drawn from the current study. It is worth noting that fractal-fractional differential operators can fastly converge the dynamics of chaotic system to its static equilibrium by adjusting the fractal and fractional parameters.

In recent years, chaos theory has risen its importance, and numerous investigations on chaotic systems have been observed. Different chaotic systems^{1,2} have been studied, particularly hidden³ and multi-stability attractors⁴. Chaos-based applications is a hot topic in science and engineering. Oscillators⁵, steganography⁶, synchronization⁷, control⁸, and parameter estimation have all employed chaotic systems. Some chaotic systems have a unique feature. They can have two or more coexisting attractors⁹. Every attractor can be achieved because of the same range of parameters, depending on the initial condition chosen. Multistable chaotic systems¹⁰ are such systems, and they have gotten a lot of attention in the recent decade because of their potential applications¹¹. Several parameters of a multistable dynamical system are particularly sensitive to noise, initial conditions, and system parameters¹². Although multi-stability makes some engineering fields more challenging, such as bridge vibration and wing design, chaotic systems with multi-stability are extremely beneficial in secure communication¹³. The appearance of hidden attractors has been associated with multi-stability¹⁴. Stable equilibrium systems and systems with hidden attractors are examples of multistable systems¹⁵. In multistable systems, self-excited attractors can be found using the typical computational process, but hidden attractors cannot be predicted through the typical computational approach¹⁶.

In recent decades, fractional calculus has been a significant mathematical technique used to represent critical challenges in various areas, including science, technology, and engineering such as, optimal power flow problems¹⁷, nonlinear output-error systems¹⁸, recommender systems with chaotic ratings behavior¹⁹, parameter estimation of nonlinear control autoregressive systems²⁰, power management involving wind-load chaos and

¹Department of Mathematics, City University of Science and Information Technology, Peshawar, Khyber Pakhtunkhwa 25000, Pakistan. ²Department of Mathematics and Physics, University of Campania "Luigi Vanvitelli", 81100 Caserta, Italy. ³Department of Mathematics, Faculty of Science, King Mongkut's University of Technology Thonburi (KMUTT), 126 Pracha Uthit Rd., Bang Mod, Thung Khru, Bangkok 10140, Thailand. ⁴Yanbu Industrial College, The Royal Commission for Jubail and Yanbu, Yanbu 30436, Saudi Arabia. ⁵Operational Research Center in Healthcare, Near East University, Near East Boulevard, 99138 Nicosia/Mersin 10, Turkey. ⁶Section of Mathematics, International Telematic University Uninettuno, Corso Vittorio Emanuele II, 39, 00186 Rome, Italy. ⁷Department of Computer Engineering, College of Computer Science, King Khalid University, Abha 61413, Saudi Arabia. ⁸Higher Institute of Applied Science and Technology of Sousse (ISSATS), University of Sousse, Cité Taffala (Ibn Khaldoun), 4003 Sousse, Tunisia. ⁹School of Mathematics and Information Science, Henan Polytechnic University, Jiaozuo 454000, China. ✉email: yaoshaowen@hpu.edu.cn

uncertainties²¹, Schrodinger equations^{22,23} and shallow water waves²⁴. The power-law function is involved in the Liouville–Caputo fractional derivative. As a result, it's common that the physical meaning of the fractional derivative is elusive or non-existent. On the other hand, many researchers identified the physical significance of fractional derivatives^{25–33}. The nonlocality property of fractional derivatives is useful in predicting certain materials' memory and heredity properties in certain circumstances. As a result, the fractional derivative^{34–37} can be defined physically as a memory search. Scholars from virtually all fields of science, technology, and engineering have been studying non-local operators of differentiation over the past few decades since they have the capability to incorporate more complex phenomena. Fractional order chaotic systems have also been a highly prominent and attractive topic in recent years. They've been studied by many researchers³⁸. Chaotic systems, particularly fractional order-based chaotic systems³⁹, have influenced attention as circuit design capability has improved with the introduction of integrated circuits⁴⁰.

The more complex the physical problems, the more complex the mathematical differentiation operators that were developed. In order to perform a single differentiation, the fractal-fractional operator combines fractional differentiation with fractal derivative. These physical processes, for example, exhibit traits of a fractal nature. There is a sort of fractal derivative that may be found in practical mathematics, and it is one in which the variable is scaled in accordance with t^a . We thought that by coming up with this nonstandard derivative, we would be able to replicate aspects of the physical world that was no longer governed by the conventional physical rules²⁶. Two parameters representing power-law, exponential decay, or Mittag–Leffler memory processes were presented by Atangana⁴¹, and the order parameter order stands for fractal derivative, which can be used to define the fractal dimension. This new set of derivatives also included an order parameter that stands for fractal derivative. Some of the previous work that has been presented in this new field has been applied either to a system of fractional ordinary differential equations or, in a few exceptional cases, to a straightforward equation for heat or diffusion^{42–47}.

Motivated from the above literature, it has been found that fractional and fractal-fractional differential operator is a best tool to include the memory effect, crossover behavior and fractal characteristics all at once. Thus, there is a need to modify the existing chaotic systems through fractional or fractal-fractional differential operators of various singular and non-singular kernels. Therefore, in this research we have considered a chaotic system which is based on a circuit design with the following considerations:

- The considered chaotic problem is modelled in terms of nonlinear system of ODEs.
- The integer ODEs system is generalized through the fractal-fractional differential operator of power law kernel.
- The system dissipation and equilibria have been calculated.
- The existence and uniqueness of the solutions have been proved.
- The Ulam stability have been proved.
- Numerical algorithm for the non-linear fractal-fractional system have been stated.
- The obtained graphical results have been portrayed through 2D and 3D phase portraits.

Mathematical preliminaries

This section provides an overview of some essential ideas and prepositions that will be used in subsequent parts of the investigation^{41,48,49}.

Definition 2.1 If $g(\tau)$ is differentiable on (a, b) with fractional order α and fractal order β and $g(\tau)$ is differentiable on the opened interval (a, b) , then the Fractal-Fractional derivative of $g(\tau)$ with fractional order α and fractal order β in Riemann–Liouville sense with power law can be written as:

$${}_{a}^{FFRL} \vartheta_{\tau}^{\alpha, \beta} g(\tau) = \frac{1}{\Gamma(m - \alpha)} \frac{d}{d\tau^{\beta}} \int_a^{\tau} g(x)(\tau - x)^{m - \alpha - 1} dx, \quad (1)$$

where $m - 1 < \alpha \leq m$, $0 < m - 1 < \beta \leq m$.

$$\frac{dg(x)}{dx^{\beta}} = \lim_{\tau \rightarrow x} \frac{f(\tau) - f(x)}{\tau^{\beta} - x^{\beta}}. \quad (2)$$

Definition 2.2 If $g(\tau)$ is fractal differentiable on (a, b) with fractal order β and $g(\tau)$ is differentiable on the opened interval (a, b) , then the Fractal-Fractional derivative of $g(\tau)$ with fractional order α and fractal order β in Caputo sense with power law is:

$${}_{a}^{FFC} \vartheta_{\tau}^{\alpha, \beta} g(\tau) = \frac{1}{\Gamma(m - \alpha)} \int_a^{\tau} \frac{dg(x)}{dx^{\beta}} (\tau - x)^{m - \alpha - 1} dx, \quad (3)$$

where $m - 1 < \alpha \leq m$, $0 < m - 1 < \beta \leq m$.

$$\frac{dg(x)}{dx^{\beta}} = \lim_{\tau \rightarrow x} \frac{f(\tau) - f(x)}{\tau^{\beta} - x^{\beta}}. \quad (4)$$

Definition 2.3 The fractal-fractional integral of Power law kernel can be expressed as follows:

$${}_0^{FFP}I_\tau^\alpha f(\tau) = \frac{\beta}{N(\alpha)} \int_0^\tau x^{\alpha-1} u(x) (\tau - x)^{\alpha-1} dx. \tag{5}$$

Definition 2.4 Numerical solution to the Caputo ODE of fractional order is defined as follows⁵⁰:
Consider nonlinear fractional ODE:

$${}_0^C \wp_\tau^\alpha z(\tau) = f(\tau, z(\tau)) \text{ with } z(0) = z_0, \tag{6}$$

The numerical algorithm for Eq. (6) is as follows:

$$z_{n+1} = z_0 + \frac{1}{\Gamma(\alpha)} \sum_{j=0}^n \left[\begin{array}{l} \frac{h^\alpha f(\tau_j, z(\tau_j))}{\alpha(\alpha + 1)} \{ (n + 1 - j)^\alpha (n + 2 - r + \alpha) - (n - j)^\alpha (n + 2 - r + 2\alpha) \} \\ - \frac{h^\alpha f(\tau_{j-1}, z(\tau_{j-1}))}{\alpha(\alpha + 1)} \{ (n + 1 - j)^{\alpha+1} - (n - j)^\alpha (n + 2 - r + \alpha) \} \end{array} \right]. \tag{7}$$

Mathematical formulation

In this study, we investigate a new type of chaotic system that was presented in⁵¹:

$$\left. \begin{array}{l} \frac{dx_1}{d\tau} = z_1, \\ \frac{dy_1}{d\tau} = -x_1 - z_1, \\ \frac{dz_1}{d\tau} = ax_1 + by_1 - z_1 + x_1y_1 - cx_1z_1 + 1, \end{array} \right\}. \tag{8}$$

with initial conditions:

$$x_1(0) = x_1^*, y_1(0) = y_1^* \text{ and } z_1(0) = z_1^*. \tag{9}$$

Here *a*, *b* and *c* are the three non-negative parameters.

The integer order system given in Eq. (8) can be transformed to the fractal-fractional order chaotic system by applying the definition given in Eq. (3). Thus, by applying the procedure given in⁴¹, Eq. (8) will take the following form:

$$\left. \begin{array}{l} {}_0^{FFP} \wp_\tau^{\alpha,\beta} z_1 = z_1, \\ {}_0^{FFP} \wp_\tau^{\alpha,\beta} (-x_1 - z_1) = -x_1 - z_1, \\ {}_0^{FFP} \wp_\tau^{\alpha,\beta} (ax_1 + by_1 - z_1 + x_1y_1 - cx_1z_1 + 1) = ax_1 + by_1 - z_1 + x_1y_1 - cx_1z_1 + 1, \end{array} \right\}. \tag{10}$$

The fractional order and fractal dimension are represented by α and β , respectively, with $0 < \alpha, \beta \leq 1$.

Dissipation and equilibria

The model in the system (8) is dissipative because:

$$\nabla V = \frac{\partial}{\partial x_1} \left(\frac{dx_1}{d\tau} \right) + \frac{\partial}{\partial y_1} \left(\frac{dy_1}{d\tau} \right) + \frac{\partial}{\partial z_1} \left(\frac{dz_1}{d\tau} \right) = -(1 + cx_1) < 0. \tag{11}$$

For the fixed points of the chaotic system (8), we consider $\frac{dx_1}{d\tau} = \frac{dy_1}{d\tau} = \frac{dz_1}{d\tau} = 0$. Hence system (8) can be written as:

$$\left. \begin{array}{l} 0 = z_1, \\ 0 = -x_1 - z_1, \\ 0 = ax_1 + by_1 - z_1 + x_1y_1 - cx_1z_1 + 1, \end{array} \right\}. \tag{12}$$

Here we have only one equilibrium point, i.e., $(x_1, y_1, z_1) = (0, -\frac{1}{b}, 0)$.

Existence and uniqueness of the fractal-fractional model

The presence of a unique solution to the fractal-fractional model, provided in Eq. (10), is established in this portion of the study. We could reformulate the Eq. (10) in the following manner because the integral is differentiable:

$$\left. \begin{array}{l} {}_0^{RL} \wp_\tau^\beta (x_1(\tau)) = \beta \tau^{\beta-1} (\Psi_1(\tau, x_1)), \\ {}_0^{RL} \wp_\tau^\beta (y_1(\tau)) = \beta \tau^{\beta-1} (\Psi_1(\tau, y_1)), \\ {}_0^{RL} \wp_\tau^\beta (z_1(\tau)) = \beta \tau^{\beta-1} (\Psi_1(\tau, z_1)). \end{array} \right\}. \tag{13}$$

where $0 < \alpha, \beta \leq 1$ and,

$$\left. \begin{aligned} \Psi_1(\tau, x_1) &= z_1, \\ \Psi_1(\tau, y_1) &= -x_1 - z_1, \\ \Psi_1(\tau, z_1) &= ax_1 + by_1 - z_1 + x_1y_1 - cx_1z_1 + 1, \end{aligned} \right\} \tag{14}$$

We can rewrite system (13) as:

$$\left. \begin{aligned} {}_0^{RL} \varphi_\tau^\alpha H(\tau) &= \beta \tau^{\beta-1} \Phi(\tau, H(\tau)), \\ H(0) &= H^* \end{aligned} \right\} \tag{15}$$

where

$$H(\tau) = \begin{cases} x_1(\tau) \\ y_1(\tau) \\ z_1(\tau) \end{cases}, \quad H(0) = \begin{cases} x_1(0) \\ y_1(0) \\ z_1(0) \end{cases}, \quad \Phi(\tau, H(0)) = \begin{cases} \Psi_1(\tau, x_1) \\ \Psi_1(\tau, y_1) \\ \Psi_1(\tau, z_1) \end{cases} \tag{16}$$

Now, by replacing ${}_0^{RL} \varphi_\tau^\alpha$ with ${}_0^C \varphi_\tau^\alpha$ and applying the fractional integral, we get:

$$H(\tau) = H(0) + \frac{\beta}{\Gamma(\alpha)} \int_a^\tau \kappa^{\beta-1} (\tau - \kappa)^{\alpha-1} \Phi(\kappa, H(\kappa)) d\kappa. \tag{17}$$

Let $P(\psi)$ be a Banach space of the real-valued continuous functions with supremum norm defined on the interval $\psi = [0, \Upsilon]$ and $\chi = P(\psi) \times P(\psi) \times P(\psi)$ with the norm $\|\Gamma\| = \sup \{|\Gamma(\tau)| : \tau \in \psi\}$.

Now, transform the problem (10) into a fixed-point problem. Define an operator $\mathbb{I} : \chi \rightarrow \chi$ as:

$$\mathbb{I}(H(\tau)) = H(0) + \frac{\beta}{\Gamma(\alpha)} \int_a^\tau \kappa^{\beta-1} (\tau - \kappa)^{\alpha-1} \Phi(\kappa, H(\kappa)) d\kappa. \tag{18}$$

For the existence theory, we use the following theorem^{52,53}.

Theorem 5.1 Assume that the operator $\mathbb{I} : \chi \rightarrow \chi$ is completely continuous and the set defined by: $\mathcal{U}(\mathbb{I}) = \{ \Phi \in \chi : H = \delta \mathbb{I}(H); \delta \in [0, 1] \}$ be bounded. Then \mathbb{I} has a fixed point χ .

Theorem 5.2 Let $\Phi : \psi \times \chi \rightarrow \mathbb{R}$ is a continuous function. Then the operator \mathbb{I} is compact.

Proof Let M be a bounded set in χ . Then there is $\vartheta_\Phi > 0$ with $|\Phi(\tau, H(\tau))| \leq \vartheta_\Phi, \forall H \in M$. So for any $H \in M$ one can get:

$$\begin{aligned} \|\mathbb{I}(H)\| &\leq \frac{\beta \vartheta_\Phi}{\Gamma(\alpha)} \max_{\tau \in \psi} \int_0^\tau \kappa^{\beta-1} (\tau - \kappa)^{\alpha-1} d\kappa, \\ &\leq \frac{\beta \vartheta_\Phi}{\Gamma(\alpha)} \max_{\tau \in \psi} \int_0^1 \varphi^{\beta-1} (1 - \varphi)^{\alpha-1} \tau^{\beta+\alpha-1} d\varphi, \\ &\leq \frac{\beta \vartheta_\Phi \Gamma^{\beta+\alpha-1}}{\Gamma(\alpha)} B(\alpha, \beta), \end{aligned} \tag{19}$$

where $B(\alpha, \beta)$ is the beta function. Thus, $M(\mathbb{I})$ it is uniformly bounded.

Next, for the equicontinuity of the operator \mathbb{I} , for any $\tau_1, \tau_2 \in \psi$ and $H \in M$, we have:

$$\begin{aligned} \|\mathbb{I}(H(\tau_1)) - \mathbb{I}(H(\tau_2))\| &\leq \frac{\beta \vartheta_\Phi}{\Gamma(\alpha)} \max_{\tau \in \psi} \left| \int_0^{\tau_1} \kappa^{\beta-1} (\tau - \kappa)^{\alpha-1} d\kappa - \int_0^{\tau_2} \kappa^{\beta-1} (\tau - \kappa)^{\alpha-1} d\kappa \right|, \\ &\leq \frac{\beta \vartheta_\Phi}{\Gamma(\alpha)} \max_{\tau \in \psi} \left(\tau_1^{\alpha+\beta-1} - \tau_2^{\alpha+\beta-1} \right) \rightarrow 0 \text{ as } \tau_1 \rightarrow \tau_2. \end{aligned} \tag{20}$$

Therefore, \mathbb{I} it is equicontinuous. Since \mathbb{I} it is a bounded and continuous operator. So, by Arzela-Ascoli theorem is completely continuous.

Theorem 5.3 Let for all $\tau \in \psi$ and $H \in \mathbb{R}$, there is a real number $\vartheta_\Phi > 0$ with $|\Phi(\tau, \mathbb{I}(\tau))| \leq \vartheta_\Phi$. Then the considered model (10) has at least one solution in the given space χ .

Proof Consider a set $\mathcal{U}(\mathbb{I}) = \{ \Phi \in \chi : H = \delta \mathbb{I}(H); \delta \in [0, 1] \}$ and show that \mathcal{U} it is bounded. Suppose $H \in \mathcal{U}$, then $H = \delta \mathbb{I}(H)$. For $\tau \in \psi$, one can easily obtain:

$$\|H\| \leq \frac{\beta \vartheta_\Phi \Gamma^{\alpha+\beta-1}}{\Gamma(\alpha)} B(\alpha, \beta). \tag{21}$$

Hence \bar{U} is bounded. So, Theorems 5.1 and 5.2 \bar{U} has at least one fixed point. Thus, the considered system (10) has at least one solution.

For further analysis, suppose the following hypothesis:

Hypothesis 5.1 There is a constant $\bar{h}_\Phi > 0$ such that for every $H, \bar{H} \in \chi$, we have:

$$|\Phi(\tau, H) - \Phi(\tau, \bar{H})| \leq \vartheta_\Phi |H - \bar{H}|. \tag{22}$$

For uniqueness, we use Banach's Contraction Theorem^{52,53}:

Theorem 5.4 Under Hypothesis 5.1 and if $\bar{\Xi} < 1$. Then the solution of the considered system (10) is unique, where

$$\bar{\Xi} = \frac{\beta \bar{h}_\Phi \Gamma^{\alpha+\beta-1}}{\Gamma(\alpha)} B(\alpha, \beta). \tag{23}$$

Proof Let we define $\max_{\tau \in \psi} |\Phi(\tau, 0)| = \omega_\Phi < \infty$ such that $\varpi \geq \frac{\beta \Gamma^{\alpha+\beta-1} B(\alpha, \beta) \omega_\Phi}{\Gamma(\alpha) - \beta \Gamma^{\alpha+\beta-1} B(\alpha, \beta) \bar{h}_\Phi}$. We show that $\bar{U}(\mathfrak{R}_\omega) \subset \mathfrak{R}_\omega$ where $\mathfrak{R}_\omega = \{H \in \chi : \|H\| \leq \omega\}$. For $H \in \mathfrak{R}_\omega$, we have:

$$\begin{aligned} \|\bar{U}(H)\| &\leq \frac{\beta}{\Gamma(\alpha)} \max_{\tau \in \psi} \int_0^\tau \kappa^{\beta-1} (\tau - \kappa)^{\alpha-1} (|\Phi(\tau, H(\tau)) - \Phi(\tau, 0)| + |\Phi(\tau, 0)|) d\kappa, \\ &\leq \frac{\beta \Gamma^{\alpha+\beta-1} B(\alpha, \beta) (\bar{h}_\Phi \|H\| + \omega_\Phi)}{\Gamma(\alpha)} \\ &\leq \frac{\beta \Gamma^{\alpha+\beta-1} B(\alpha, \beta) (\bar{h}_\Phi \varpi + \omega_\Phi)}{\Gamma(\alpha)} \\ &\leq \bar{\Xi}. \end{aligned} \tag{24}$$

Let the operator $\bar{U} : \chi \rightarrow \chi$ define it by (18). Then in view of Hypothesis 5.1, for every $\tau \in \psi$ and for every $H, \bar{H} \in \chi$, we have:

$$\begin{aligned} \|\bar{U}(H) - \bar{U}(\bar{H})\| &\leq \frac{\beta}{\Gamma(\alpha)} \max_{\tau \in \psi} \left| \int_0^\tau \kappa^{\beta-1} (\tau - \kappa)^{\alpha-1} \Phi(\kappa, H(\kappa)) d\kappa - \int_0^\tau \kappa^{\beta-1} (\tau - \kappa)^{\alpha-1} \Phi(\kappa, \bar{H}(\kappa)) d\kappa \right| \\ &\leq \omega \|H - \bar{H}\|. \end{aligned} \tag{25}$$

Hence \bar{U} is a contraction from (25). Thus, the integral Eq. (17) has a unique solution, and so does the system (10) has a unique solution.

Ulam stability

In this section, we develop and present some results on the stability of the model (10). We will consider a small perturbation $\Upsilon \in P(\psi)$ that depends only on the solution and $\Upsilon(0) = 0$. Further:

$$|\Upsilon(\tau)| \leq \varepsilon, \text{ for } \varepsilon > 0, \tag{26}$$

$${}^{FFP} \mathcal{I}_\tau^{\alpha, \beta} (H(\tau)) = \Phi(\tau, H(\tau)) + \Upsilon(\tau). \tag{27}$$

Lemma 6.1 The modified problem's solution is as follows:

$$\begin{cases} {}^{FFP} \mathcal{I}_\tau^{\alpha, \beta} (H(\tau)) = \Phi(\tau, H(\tau)) + \Upsilon(\tau), \\ H(0) = H^*, \end{cases} \tag{28}$$

Satisfies the following relation:

$$\left| H(\tau) - \left(H(0) + \frac{\beta}{\Gamma(\alpha)} \int_a^\tau \kappa^{\beta-1} (\tau - \kappa)^{\alpha-1} \Phi(\kappa, H(\kappa)) d\kappa \right) \right| \leq \left(\frac{\beta \Gamma^{\alpha+\beta-1}}{\Gamma(\alpha)} B(\alpha, \beta) \right) \varepsilon = \mathbb{C}_{\alpha, \beta} \varepsilon. \tag{29}$$

Theorem 6.1 Under Hypothesis 5.1 and Lemma 6.1, the integral Eq. (17) solution is Ulam-Hyers stable. Consequently, the considered system is Ulam-Hyers stable if $\Xi < 1$, where Ξ is given by (23).

Proof Suppose $K \in \chi$ be a unique solution and $H \in \chi$ be any solution of (10), then:

$$\begin{aligned}
 |H(\tau) - K(\tau)| &= \left| H(\tau) - \left(K(0) + \frac{\beta}{\Gamma(\alpha)} \int_a^\tau \kappa^{\beta-1} (\tau - \kappa)^{\alpha-1} \Phi(\kappa, K(\kappa)) d\kappa \right) \right| \\
 &\leq \left| H(\tau) - \left(H(0) + \frac{\beta}{\Gamma(\alpha)} \int_a^\tau \kappa^{\beta-1} (\tau - \kappa)^{\alpha-1} \Phi(\kappa, H(\kappa)) d\kappa \right) \right| \\
 &\quad + \left| H \left(H(0) + \frac{\beta}{\Gamma(\alpha)} \int_a^\tau \kappa^{\beta-1} (\tau - \kappa)^{\alpha-1} \Phi(\kappa, H(\kappa)) d\kappa \right) \right. \\
 &\quad \left. - \left(K(0) + \frac{\beta}{\Gamma(\alpha)} \int_a^\tau \kappa^{\beta-1} (\tau - \kappa)^{\alpha-1} \Phi(\kappa, K(\kappa)) d\kappa \right) \right| \\
 &\leq C_{\alpha,\beta} \varepsilon + \frac{\beta \hbar \Phi \Gamma^{\alpha+\beta-1}}{\Gamma(\alpha)} B(\alpha, \beta) \|H - K\|.
 \end{aligned}
 \tag{30}$$

We can write the above inequality as:

$$|H(\tau) - K(\tau)| \leq C_{\alpha,\beta} \varepsilon + \Xi \|H - K\|.$$
(31)

From (31), we can write:

$$|H(\tau) - K(\tau)| \leq \left(\frac{C_{\alpha,\beta}}{1 - \Xi} \right) \varepsilon.$$
(32)

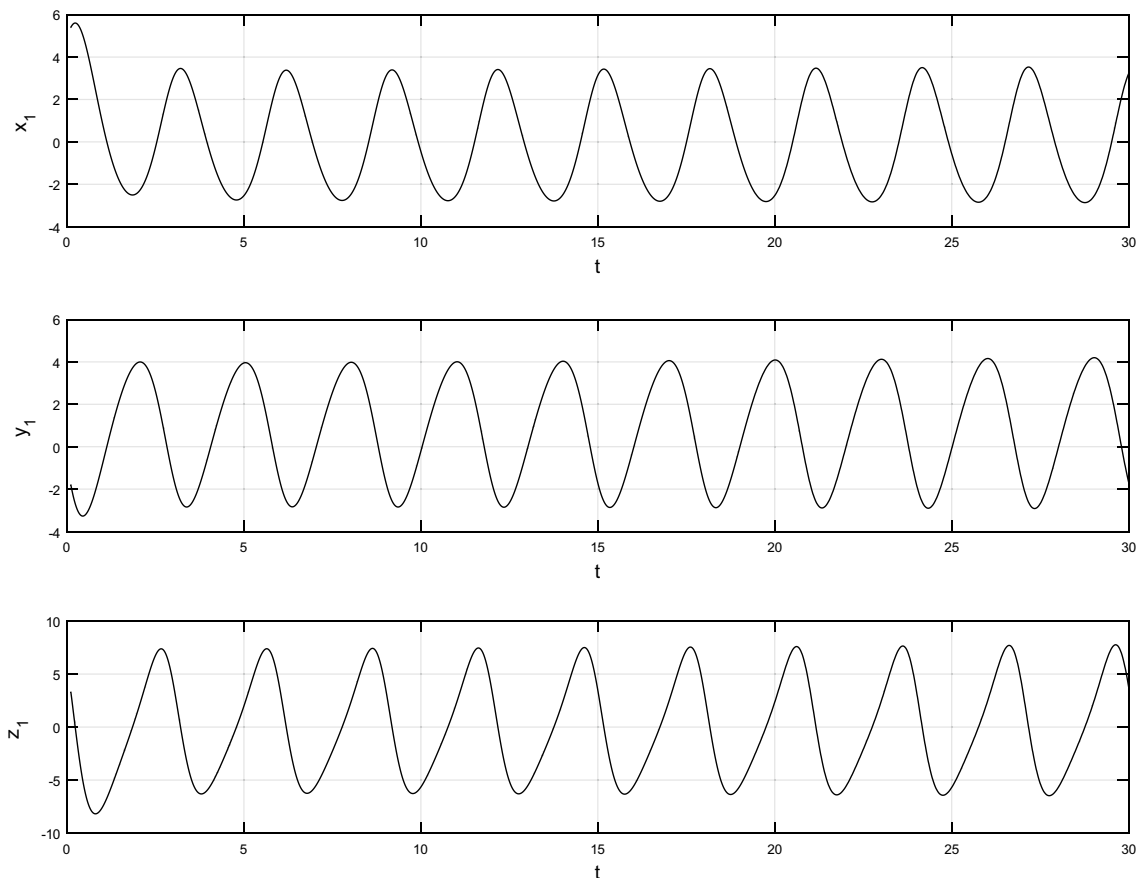


Figure 1. The classical case’s chaotic attractor dynamics i.e., $\alpha = \beta = 1$.

Therefore, the result (32) concludes that the solution of (10) is Ulam-Hyers stable, and therefore this supposed problem is Ulam-Hyers stable as well.

Numerical scheme for the fractal-fractional model

Consider the system (10)

$$\left. \begin{aligned} {}^{RL}_0 \wp_\tau^\alpha(x_1(\tau)) &= \beta\tau^{\beta-1}(\Phi_1(\tau, y_1)), \\ {}^{RL}_0 \wp_\tau^\alpha(y_1(\tau)) &= \beta\tau^{\beta-1}(\Phi_2(\tau, y_2)), \\ {}^{RL}_0 \wp_\tau^\alpha(z_1(\tau)) &= \beta\tau^{\beta-1}(\Phi_3(\tau, y_3)). \end{aligned} \right\} \quad (33)$$

We can also write:

$$\left. \begin{aligned} {}^C_0 \wp_t^\alpha(x_1(\tau)) &= \Theta_1(\tau, x_1), \\ {}^C_0 \wp_t^\alpha(y_1(\tau)) &= \Theta_2(\tau, y_1), \\ {}^C_0 \wp_t^\alpha(z_1(\tau)) &= \Theta_3(\tau, z_1). \end{aligned} \right\} \quad (34)$$

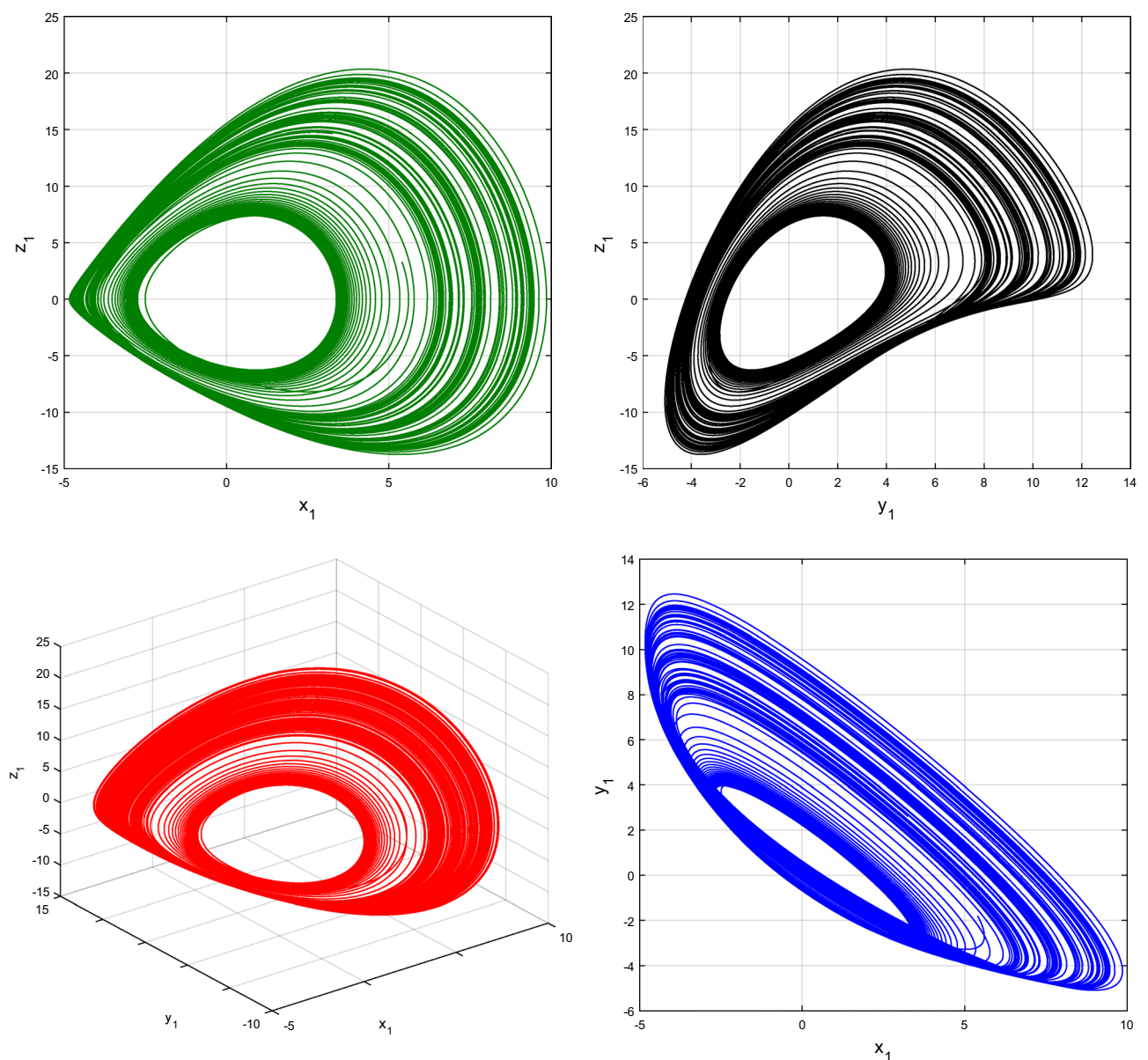


Figure 2. Classical systems' 2D and 3D phase portraits of the chaotic attractor dynamics case i.e., $\alpha = \beta = 1$.

Now by replacing ${}^RL_0 \mathcal{D}_t^\alpha$ with ${}^C_0 \mathcal{D}_t^\alpha$ and applying the procedure given in Eq. (7), we obtain the numerical algorithm in the following form:

$$x_1(\tau_{n+1}) = x_1(\tau_0) + \frac{1}{\Gamma(\alpha)} \sum_{j=0}^n \left[\frac{h^\alpha \Theta_1(\tau_j, x_1(\tau_j))}{\alpha(\alpha+1)} \{ (n+1-j)^\alpha (n+2-r+\alpha) - (n-j)^\alpha (n+2-r+2\alpha) \} \right. \\ \left. - \frac{h^\alpha \Theta_1(\tau_{j-1}, x_1(\tau_{j-1}))}{\alpha(\alpha+1)} \{ (n+1-j)^{\alpha+1} - (n-j)^\alpha (n+2-r+\alpha) \} \right], \tag{35}$$

$$y_1(\tau_{n+1}) = y_1(\tau_0) + \frac{1}{\Gamma(\alpha)} \sum_{j=0}^n \left[\frac{h^\alpha \Theta_2(\tau_j, y_1(\tau_j))}{\alpha(\alpha+1)} \{ (n+1-j)^\alpha (n+2-r+\alpha) - (n-j)^\alpha (n+2-r+2\alpha) \} \right. \\ \left. - \frac{h^\alpha \Theta_2(\tau_{j-1}, y_1(\tau_{j-1}))}{\alpha(\alpha+1)} \{ (n+1-j)^{\alpha+1} - (n-j)^\alpha (n+2-r+\alpha) \} \right], \tag{36}$$

$$z_1(\tau_{n+1}) = z_1(\tau_0) + \frac{1}{\Gamma(\alpha)} \sum_{j=0}^n \left[\frac{h^\alpha \Theta_3(\tau_j, z_1(\tau_j))}{\alpha(\alpha+1)} \{ (n+1-j)^\alpha (n+2-r+\alpha) - (n-j)^\alpha (n+2-r+2\alpha) \} \right. \\ \left. - \frac{h^\alpha \Theta_3(\tau_{j-1}, z_1(\tau_{j-1}))}{\alpha(\alpha+1)} \{ (n+1-j)^{\alpha+1} - (n-j)^\alpha (n+2-r+\alpha) \} \right]. \tag{37}$$

Discussion and results

This section of the article contains graphical representations of the results obtained from the recent study. This study offers the dynamics of a newly designed circuit under the consideration of fractal-fractional derivative of power law kernel. The problem has been analyzed for both fractional order parameter α and fractal dimension β . Simulations are performed and results are computed using MATLAB software. For the initial values, we have considered $x_1(0) = 5.4$, $y_1(0) = -1.8$ and $z_1(0) = 3.3$ while $a = 0.1$, $b = 5$ and $c = 0.3$.

Using $\alpha = \beta = 1$ and keeping the other variables constant, Figs. 1 and 2 illustrate the classical behavior of a chaotic attractor. The influence that the fractional parameter α has on the chaotic attractor behavior is seen in Figs. 3, 4, 5, 6, 7, 8. As seen in Figs. 3 and 4, the dynamics converges to its static equilibrium when fractional parameter α is reduced while in the classical/integer order, it always evolve around its equilibrium. Further, it

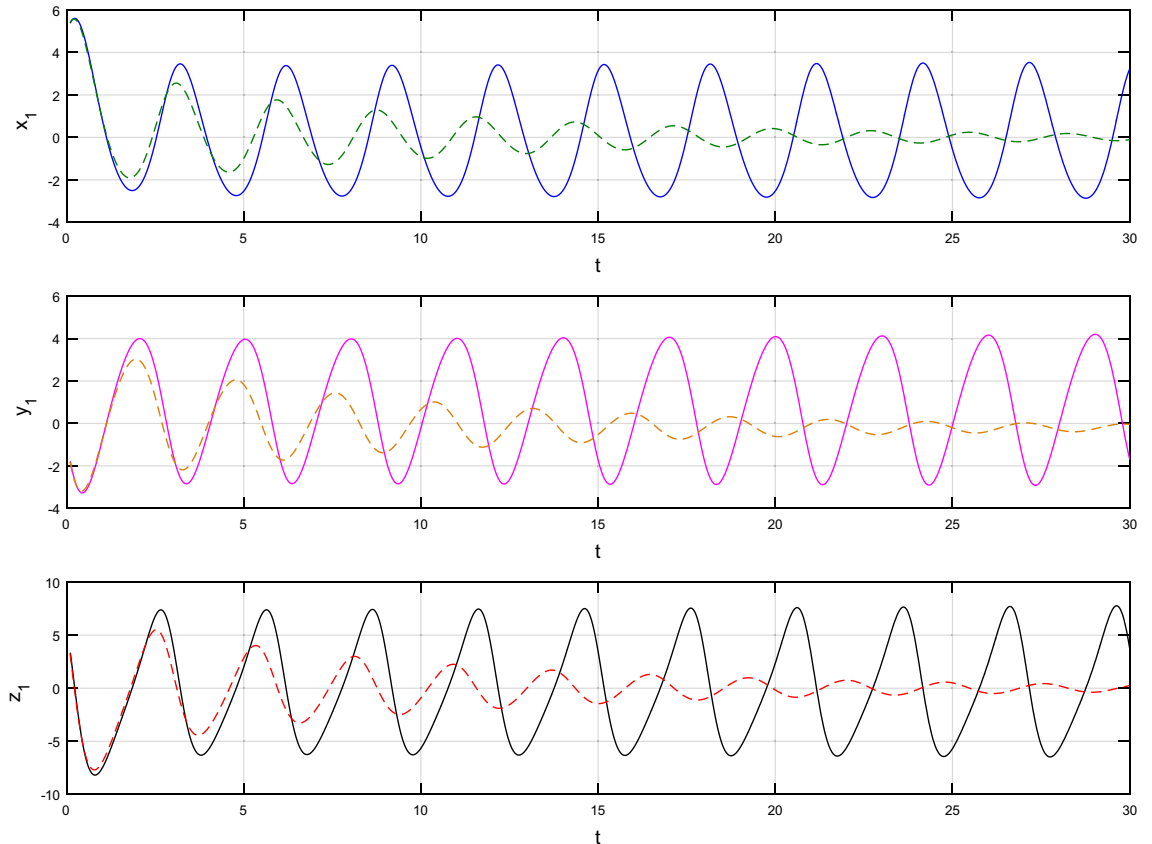


Figure 3. An analysis of the chaotic attractors for this case when $\alpha = 1$ (line) and $\alpha = 0.95$ (dash).

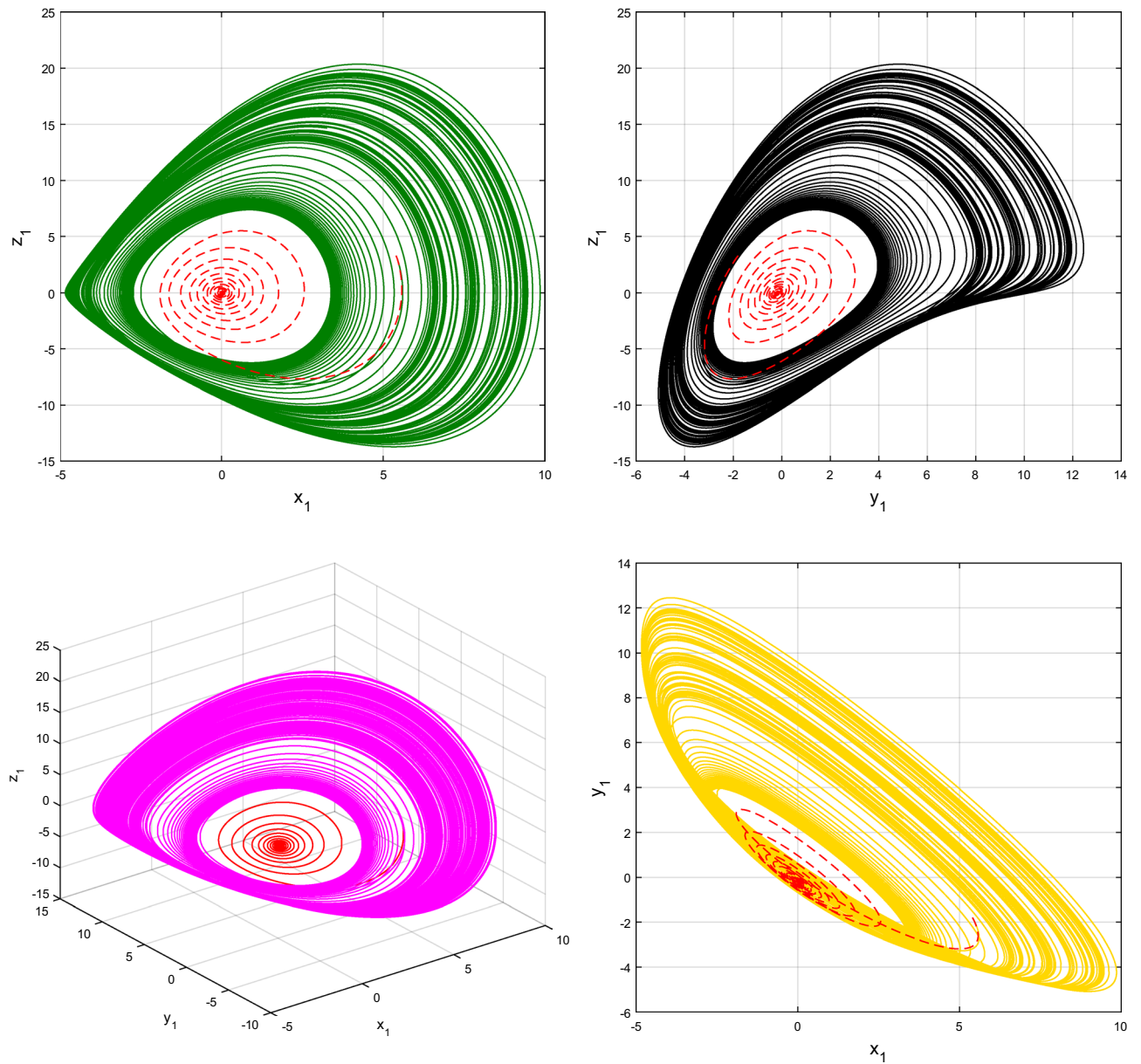


Figure 4. The case's chaotic attractor dynamics, shown in 2D and 3D phase portraits when $\alpha = 1$ (line) and $\alpha = 0.95$ (dash).

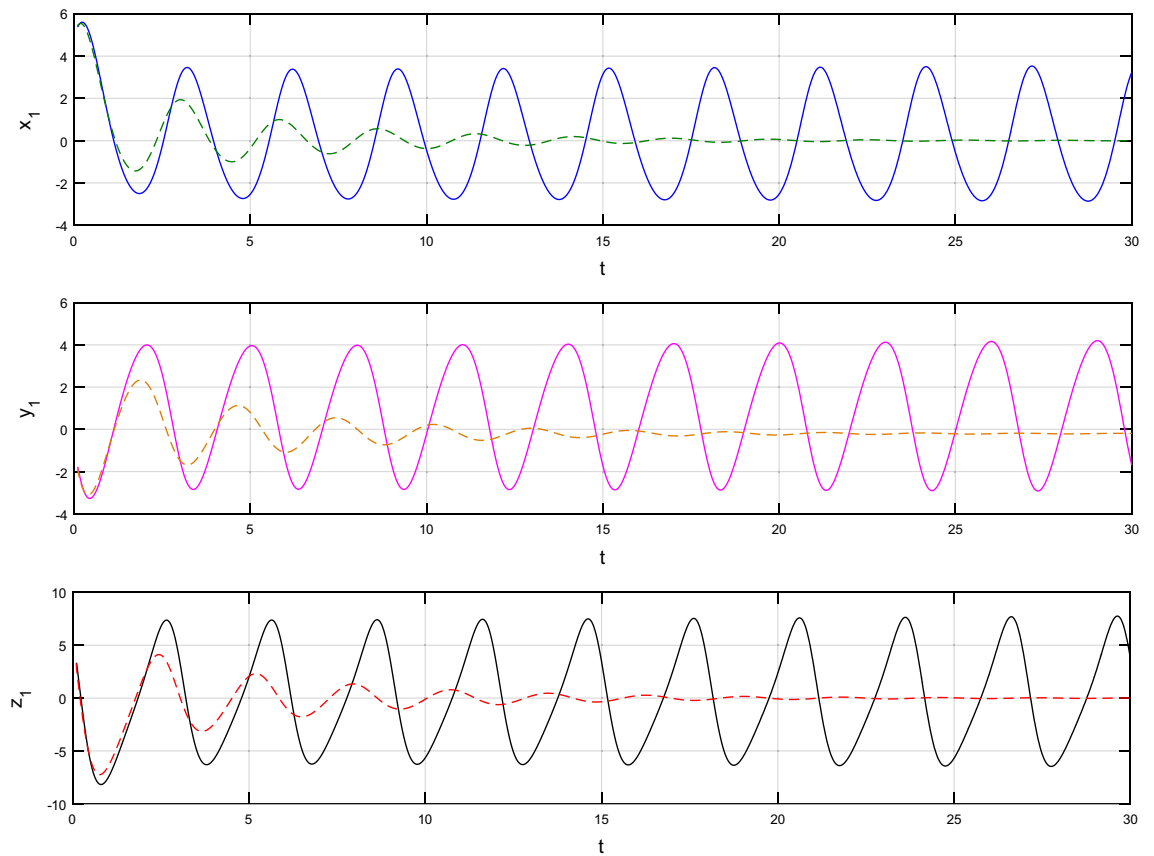


Figure 5. An analysis of the chaotic attractors for this case when $\alpha=1$ (line) and $\alpha=0.90$ (dash).

can be noticed that the time period and amplitude of the oscillations reduces by reducing α . The impact α on the dynamic of chaotic attractors conforms to the same configuration as that which is shown in Figs. 5, 6, 7, 8. From the figures depicting the effects of effect α on chaotic attractors, perhaps the current fractal-fractional theory provides us with several solutions, rather than one as in classical/integer order. It provides us an alternative, and if we make the necessary adjustments, we may be able to get the best outcome possible by combining the results of our experiments with the theoretical data. Figures 9, 10, 11, 12, 13, 14 illustrates the effect that the fractal

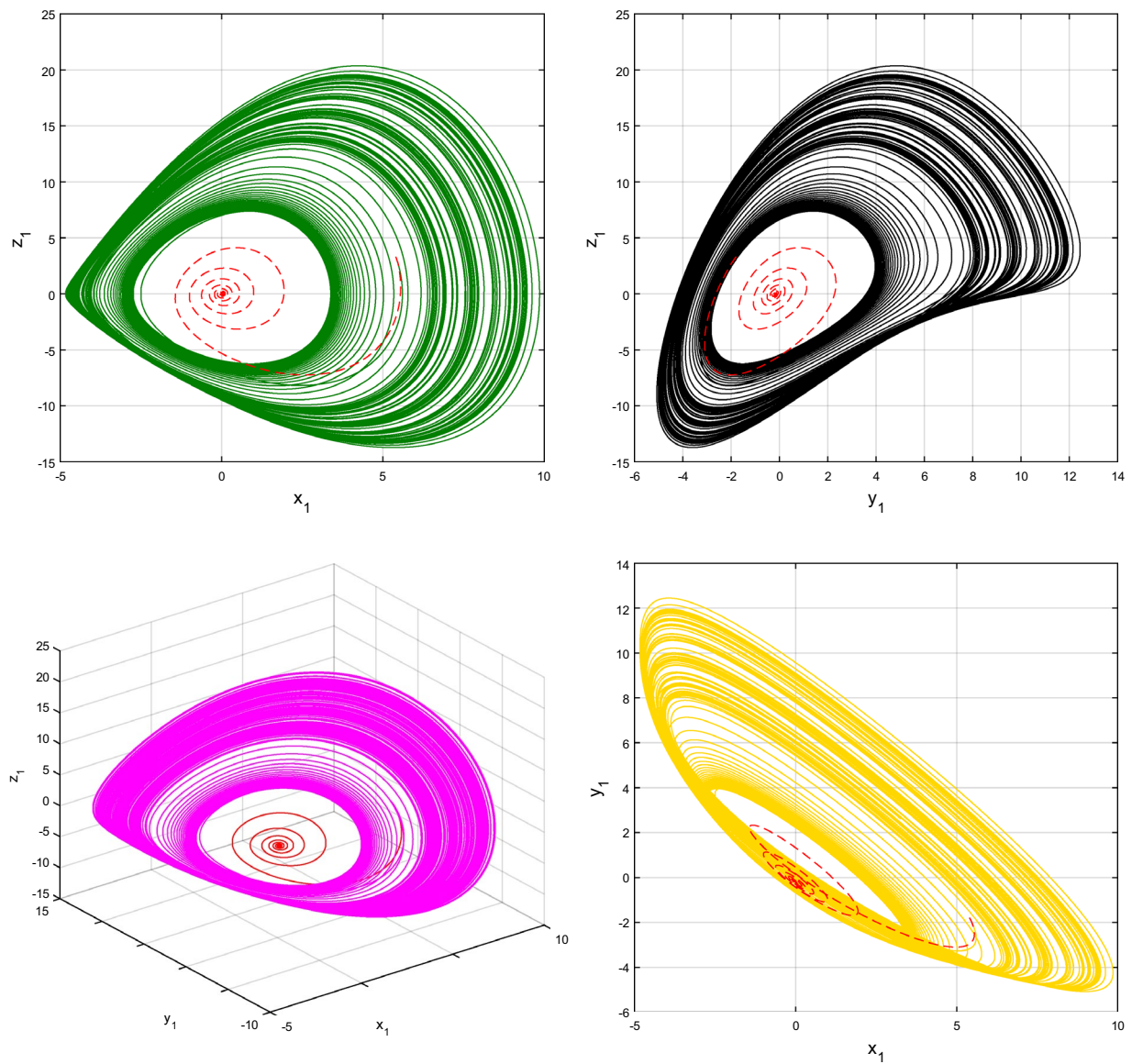


Figure 6. The case's chaotic attractor dynamics, shown in 2D and 3D phase portraits when $\alpha = 1$ (line) and $\alpha = 0.90$ (dash).

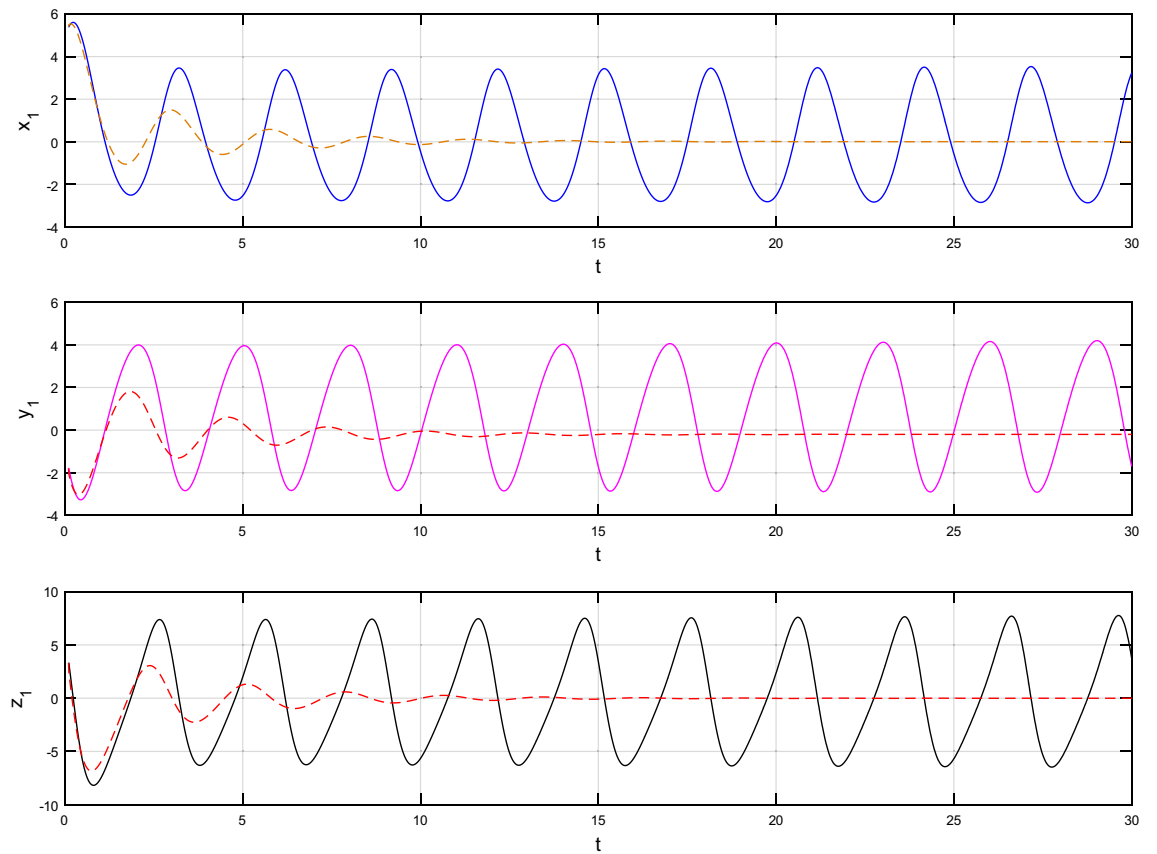


Figure 7. An analysis of the chaotic attractors for this case when $\alpha = 1$ (line) and $\alpha = 0.85$ (dash).

dimension β has on the dynamics of chaotic attractors. We made the observation that decreasing the value of the fractal dimension parameter β causes the chaotic attractor dynamics to persist for a longer period of time while the amplitude approximately remains the same. There are various 2D and 3D phase graphs produced in order to better understand the dynamical behavior of the considered chaotic system. For the purpose of making the differences between them more evident, we compare each figure to the classical order. We can observe the dynamics of the problem-limited cycles and periodic orbits that have been described based on the graphs that have been displayed so far.

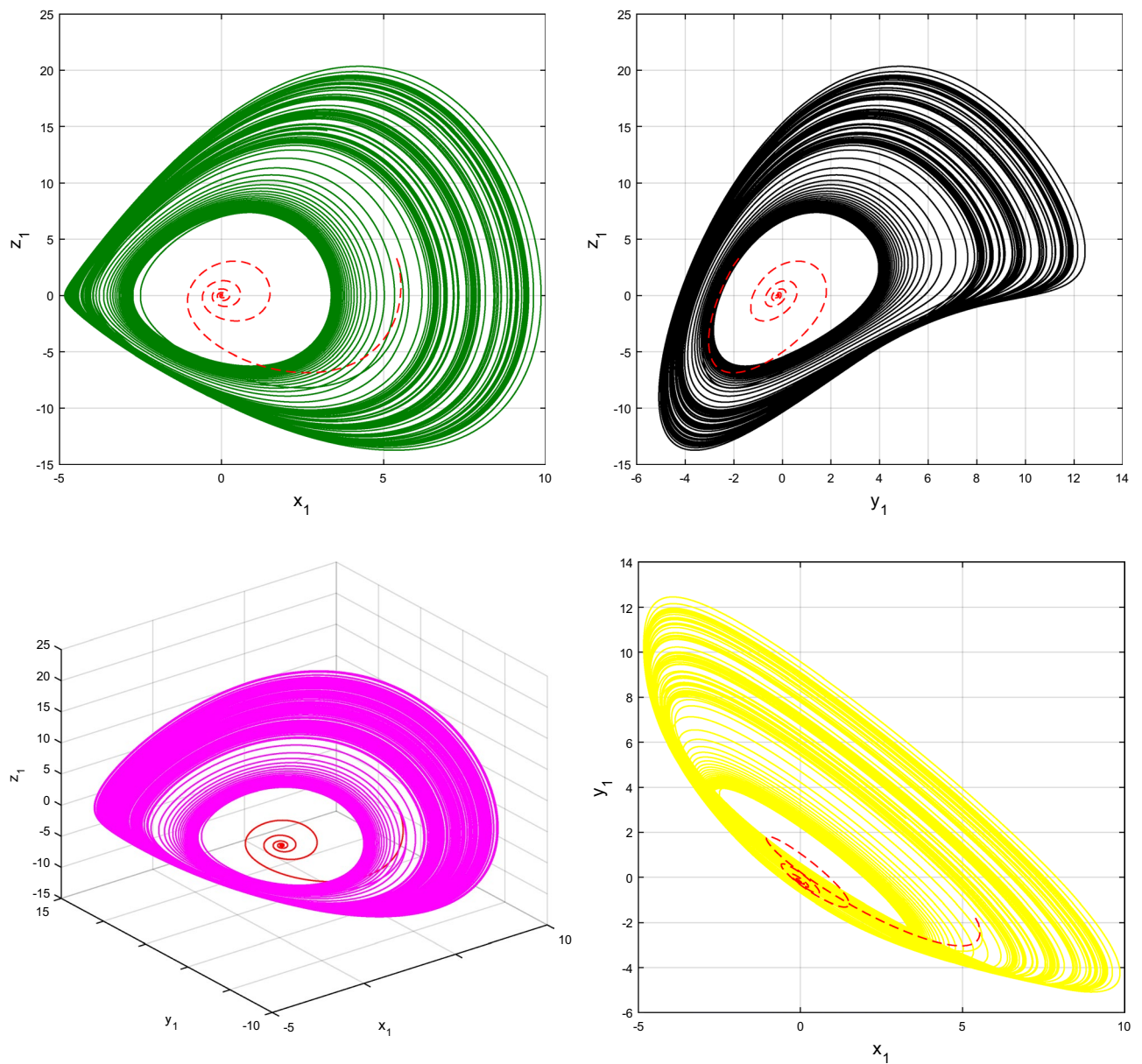


Figure 8. The case's chaotic attractor dynamics, shown in 2D and 3D phase portraits when $\alpha = 1$ (line) and $\alpha = 0.85$ (dash).

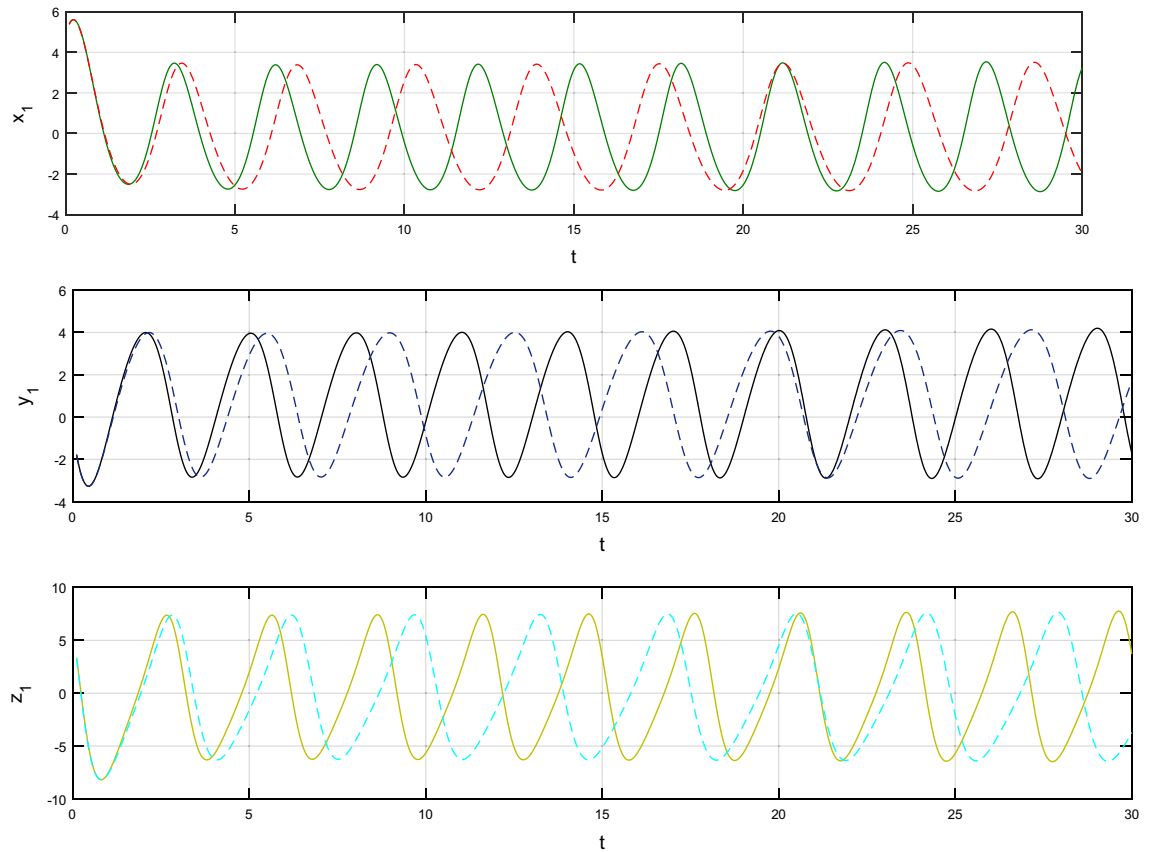


Figure 9. An analysis of the chaotic attractors for this case when $\beta=1$ (line) and $\beta=0.95$ (dash).

Concluding remarks

This study has been carried out for the chaotic system based on circuit design presented by a three-dimensional chaotic system. The problem is modelled in the form of nonlinear integer order ODEs along with the initial conditions. In addition, theoretical analyses of the problem such as equilibria and dissipation have been calculated while the existence and uniqueness of the solutions have been proved. In order to generalize the classical model, we used a fractal-fractional differential operator of power law. To get the graphical solution, a numerical approach is also stated, after which it is implemented using the MATLAB software for simulations. Several graphs are used to illustrate the strange attractors that the chaotic system produces.

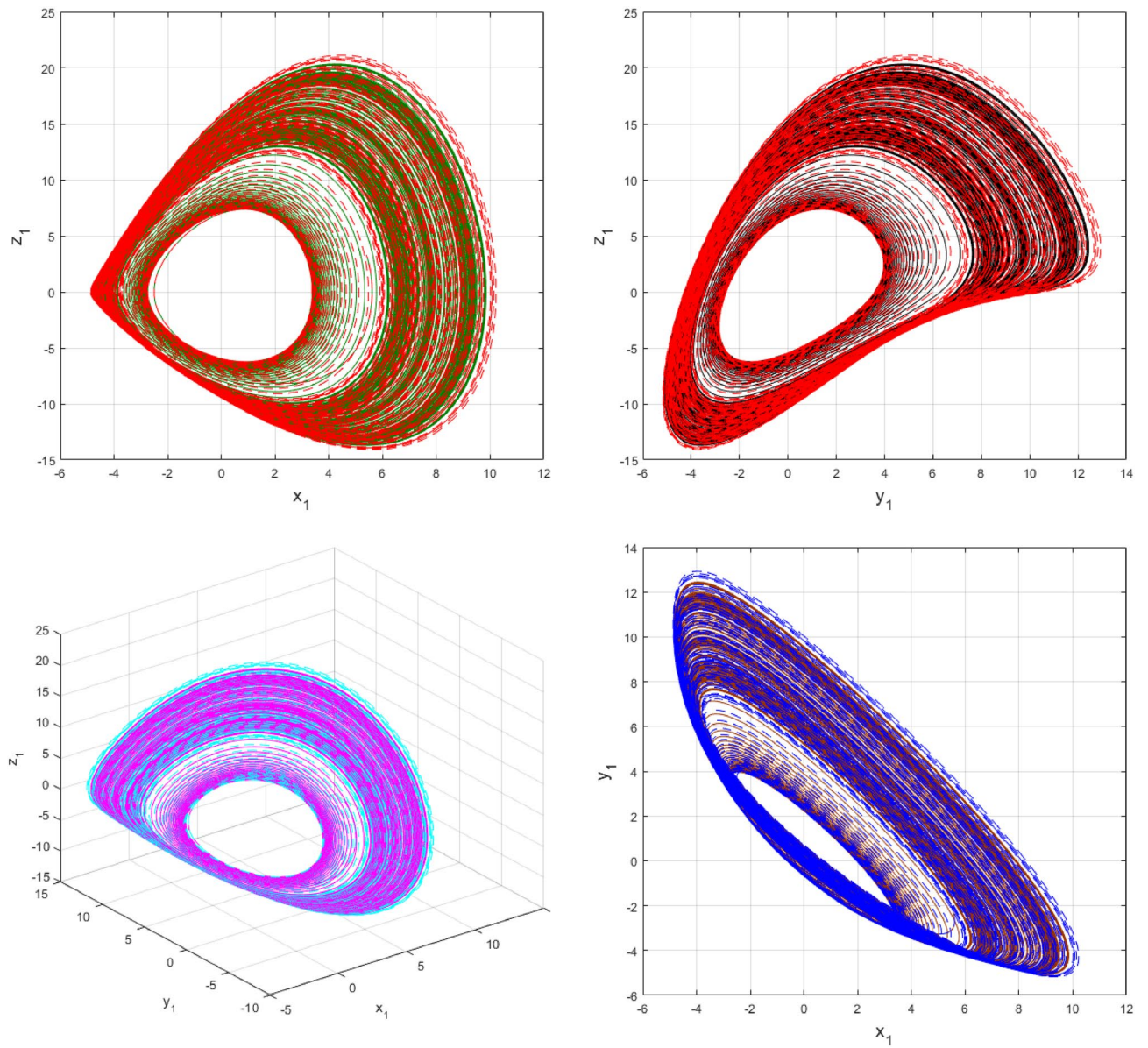


Figure 10. The case's chaotic attractor dynamics, shown in 2D and 3D phase portraits when $\beta=1$ (line) and $\beta=0.95$ (dash).

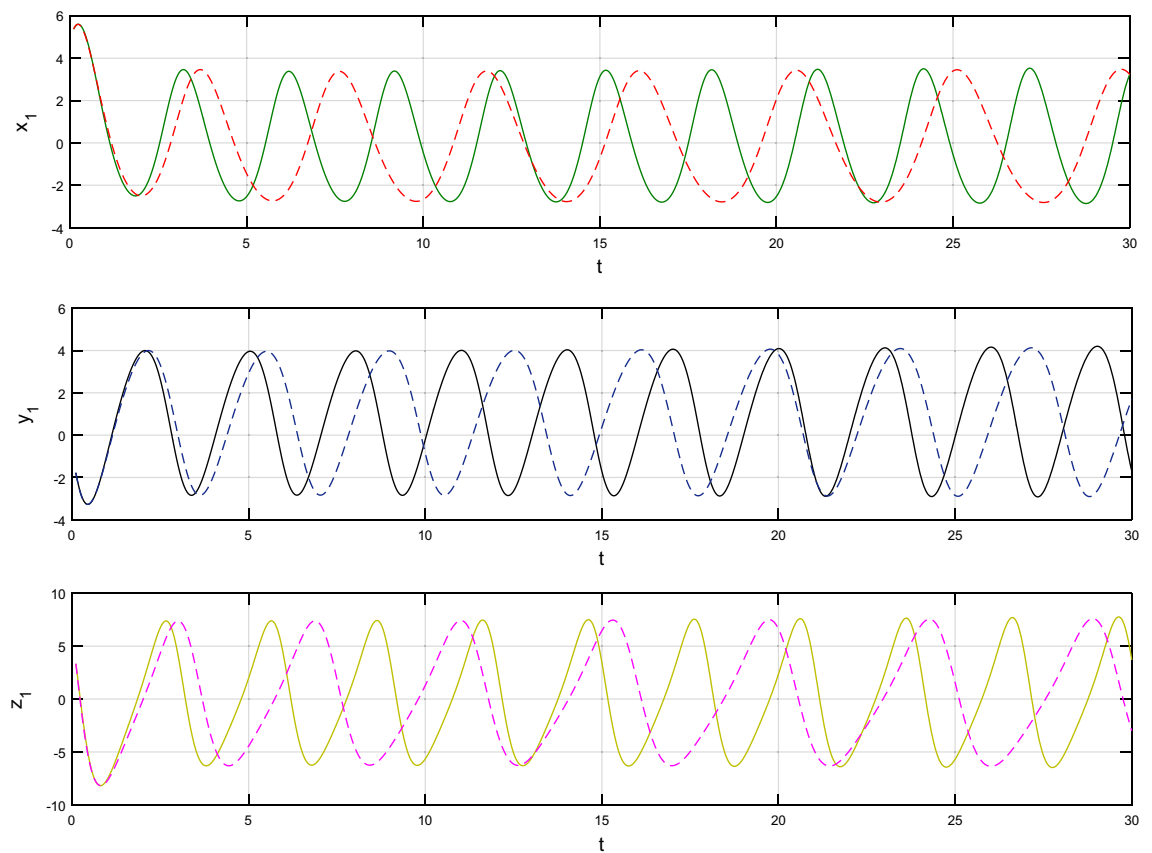


Figure 11. An analysis of the chaotic attractors for this case when $\beta=1$ (line) and $\beta=0.90$ (dash).

According to our observations, the chaotic system exhibits certain unusual behaviors as it fluctuates. Because of this, the outcomes of the current model can be significantly changed, and since fractional-order parameters and fractal dimensions are involved in the current study to make it more general. In addition, it is obvious from the figures shown above that a reduction in fractional parameter α will result in decrease in amplitude as well as

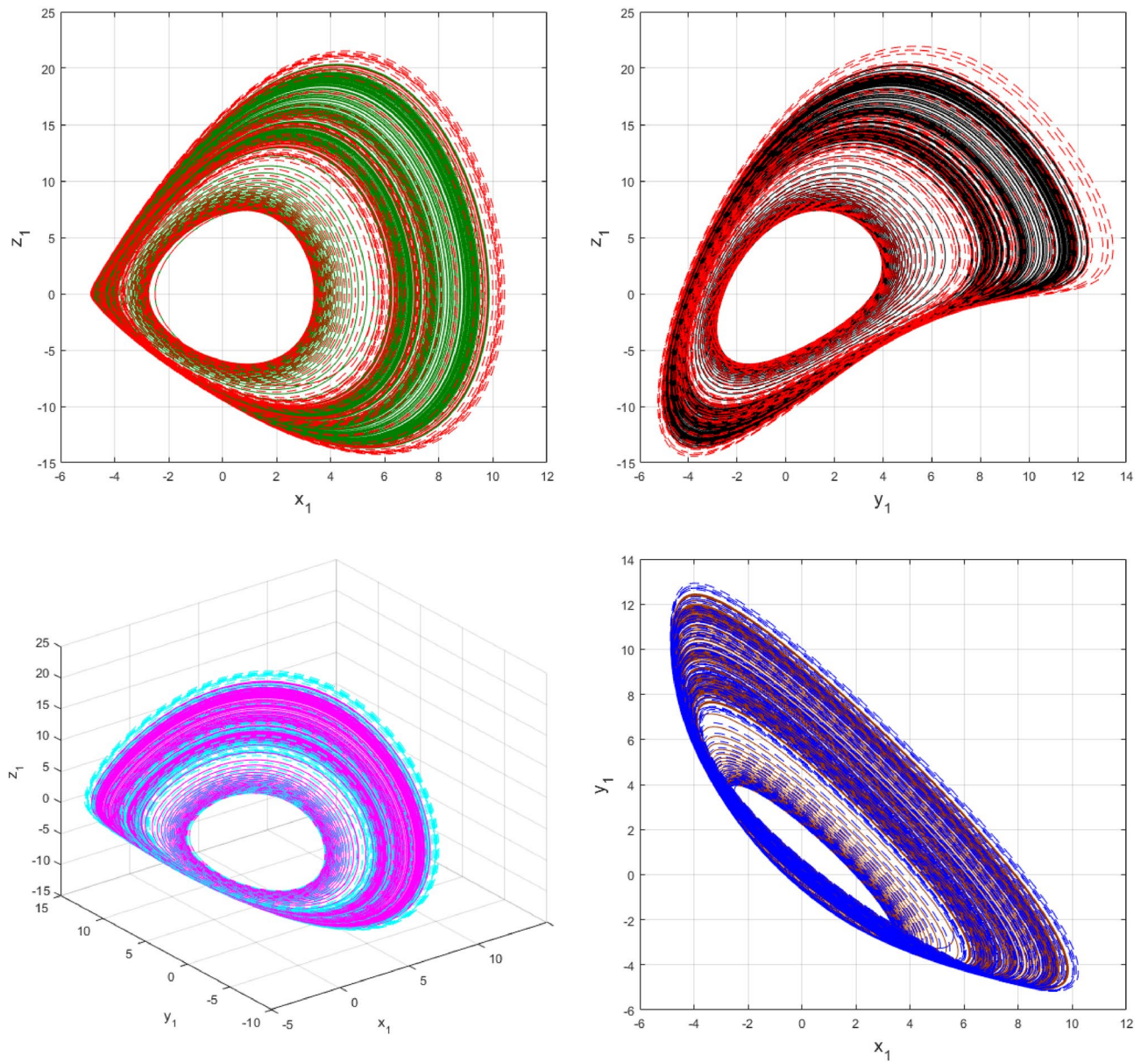


Figure 12. The case's chaotic attractor dynamics, shown in 2D and 3D phase portraits when $\beta=1$ (line) and $\beta=0.90$ (dash).

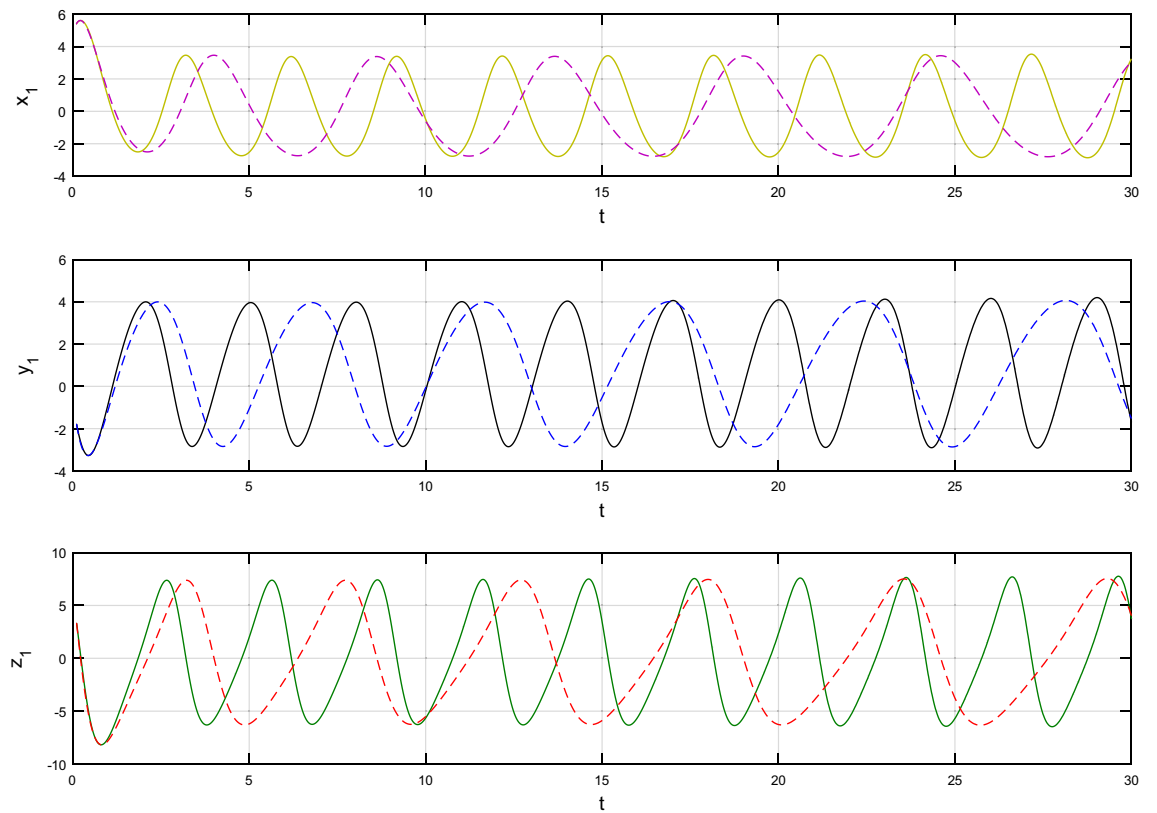


Figure 13. An analysis of the chaotic attractors for this case when $\beta=1$ (line) and $\beta=0.85$ (dash).

time period of oscillations while a decrease in fractal parameter β would result in increase in the periods of the trajectories. Modifying these parameters is most likely to produce results that are comparable to those obtained numerically with the experimental results. It is noteworthy to notice that, when $\alpha = \beta = 1$, we may recover the integer order results from the modified fractal-fractional one.

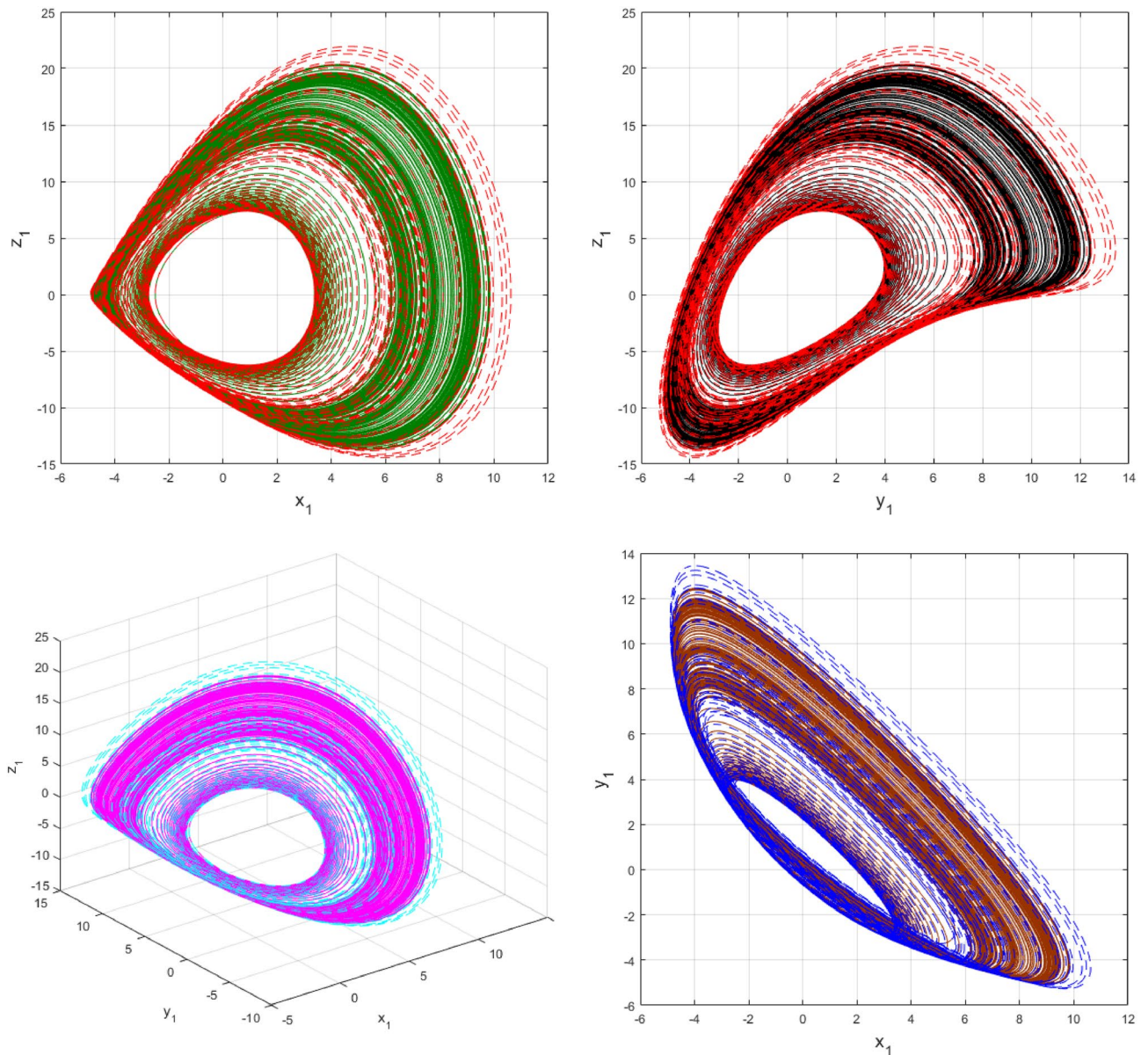


Figure 14. The case's chaotic attractor dynamics, shown in 2D and 3D phase portraits when $\beta=1$ (line) and $\beta=0.85$ (dash).

Data availability

The data will be available from the corresponding author upon request.

Received: 20 November 2022; Accepted: 22 March 2023

Published online: 28 March 2023

References

1. Akgul, A., Calgan, H., Koyuncu, I., Pehlivan, I. & Istanbulu, A. Chaos-based engineering applications with a 3D chaotic system without equilibrium points. *Nonlinear Dyn.* **2**, 481–495 (2016).
2. Ahmad, Z., Ali, F., Khan, N. & Khan, I. Dynamics of fractal-fractional model of a new chaotic system of integrated circuit with Mittag-Leffler kernel. *Chaos Solitons Fractals* **153**, 111602 (2021).
3. Wei, Z., Moroz, I., Sprott, J. C., Wang, Z. & Zhang, W. Detecting hidden chaotic regions and complex dynamics in the self-exciting homopolar disc dynamo. *Int. J. Bifurcation Chaos* <https://doi.org/10.1142/S021812741730008727> (2017).
4. Rajagopal, K., Jafari, S., Akgul, A. & Karthikeyan, A. Modified jerk system with self-exciting and hidden flows and the effect of time delays on existence of multi-stability. *Nonlinear Dyn.* **93**, 1087–1108 (2018).
5. Hu, W., Akgul, A., Li, C., Zheng, T. & Li, P. A switchable chaotic oscillator with two amplitude-frequency controllers. *J. Circuits Syst. Comput.* <https://doi.org/10.1142/S021812661750158426> (2017).
6. Vaidyanathan, S., Akgul, A., Kaçar, S. & Çavuşoğlu, U. A new 4-D chaotic hyperjerk system, its synchronization, circuit design and applications in RNG, image encryption and chaos-based steganography. *Eur. Phys. J. Plus* **133**(2), 1–18 (2018).

7. Lai, Q., Akgul, A., Varan, M., Kengne, J. & TuranErguzel, A. Dynamic analysis and synchronization control of an unusual chaotic system with exponential term and coexisting attractors. *Chin. J. Phys.* **56**, 2837–2851 (2018).
8. Wang, X., Akgul, A., Cicek, S., Pham, V. T. & Hoang, D. V. A chaotic system with two stable equilibrium points: Dynamics. *Circuit Realization Commun. Appl.* <https://doi.org/10.1142/S021812741750130927> (2017).
9. Jafari, S., Rajagopal, K., Hayat, T., Alsaedi, A. & Pham, V. T. Simplest megastable chaotic oscillator. *Int. J. Bifurcation Chaos* <https://doi.org/10.1142/S021812741950187629> (2019).
10. Bao, B. C., Bao, H., Wang, N., Chen, M. & Xu, Q. Hidden extreme multistability in memristive hyperchaotic system. *Chaos, Solitons Fractals* **94**, 102–111 (2017).
11. Vaidyanathan, S. *et al.* Multistability in a novel chaotic system with perpendicular lines of equilibrium: analysis, adaptive synchronization and circuit design.
12. Chudzik, A., Perlikowski, P., Stefanski, A. & Kapitaniak, T. Multistability and rare attractors in van der Pol–Duffing oscillator. *Int. J. Bifurcation Chaos* **21**, 1907–1912. <https://doi.org/10.1142/S0218127411029513> (2011).
13. Natiq, H., Ariffin, M. R. K., Asbullah, M. A., Mahad, Z. & Najah, M. Enhancing chaos complexity of a plasma model through power input with desirable random features. *Entropy* **23**, 48 (2020).
14. Peng, G. & Min, F. Multistability analysis, circuit implementations and application in image encryption of a novel memristive chaotic circuit. *Nonlinear Dyn.* **90**, 1607–1625 (2017).
15. Faghani, Z., Nazarimehr, F., Jafari, S. & Sprott, J. C. A new category of three-dimensional chaotic flows with identical eigenvalues. *Int. J. Bifurcation Chaos* <https://doi.org/10.1142/S021812742050026130> (2020).
16. Lai, Q. & Chen, S. Generating multiple chaotic attractors from Sprott B system. *Int. J. Bifurcation Chaos* <https://doi.org/10.1142/S021812741650177726> (2016).
17. Muhammad, Y. *et al.* Design of fractional comprehensive learning PSO strategy for optimal power flow problems. *Appl. Soft Comput.* **130**, 109638 (2022).
18. Chaudhary, N. I. *et al.* Design of auxiliary model based normalized fractional gradient algorithm for nonlinear output-error systems. *Chaos Solitons Fractals* **163**, 112611 (2022).
19. Khan, Z. A., Chaudhary, N. I. & Raja, M. A. Z. Generalized fractional strategy for recommender systems with chaotic ratings behavior. *Chaos Solitons Fractals* **160**, 112204 (2022).
20. Malik, M. F. *et al.* Swarming intelligence heuristics for fractional nonlinear autoregressive exogenous noise systems. *Chaos Solitons Fractals* **167**, 113085 (2023).
21. Muhammad, Y. *et al.* Fractional memetic computing paradigm for reactive power management involving wind-load chaos and uncertainties. *Chaos Solitons Fractals* **161**, 112285 (2022).
22. Rizvi, S. T. R. *et al.* Various optical soliton for a weak fractional nonlinear Schrödinger equation with parabolic law. *Results Phys.* **23**, 103998 (2021).
23. Rizvi, S. T. R., Seadawy, A. R., Ahmed, S., Younis, M. & Ali, K. Study of multiple lump and rogue waves to the generalized unstable space time fractional nonlinear Schrödinger equation. *Chaos Solitons Fractals* **151**, 111251 (2021).
24. Younis, M. *et al.* Nonlinear dynamical study to time fractional Dullian–Gottwald–Holm model of shallow water waves. *Int. J. Mod. Phys. B* <https://doi.org/10.1142/S0217979222500047> (2021).
25. Ali, F., Ahmad, Z., Arif, M., Khan, I. & Nisar, K. S. A time fractional model of generalized Couette flow of couple stress nanofluid with heat and mass transfer: Applications in engine oil. *IEEE Access* **8**, 146944–146966 (2020).
26. Ahmad, Z., Ali, F., Alqahtani, A. M., Khan, N. & Khan, I. Dynamics of cooperative reactions based on chemical kinetics with reaction speed: A comparative analysis with singular and nonsingular kernels. *Fractals* <https://doi.org/10.1142/S0218348X22400485> (2021).
27. Khan, N. *et al.* Maxwell nanofluid flow over an infinite vertical plate with ramped and isothermal wall temperature and concentration. *Math. Probl. Eng.* **2021**, 1–19 (2021).
28. Ali, F., Haq, F., Khan, N., Imtiaz, A. & Khan, I. A time fractional model of hemodynamic two-phase flow with heat conduction between blood and particles: Applications in health science. *Waves Random Complex Media* <https://doi.org/10.1080/17455030.2022.2100002> (2022).
29. Shah, J. *et al.* MHD flow of time-fractional Casson nanofluid using generalized Fourier and Fick’s laws over an inclined channel with applications of gold nanoparticles. *Sci. Rep.* **12**, 1–16 (2022).
30. Murtaza, S., Kumam, P., Kaewkhao, A., Khan, N. & Ahmad, Z. Fractal fractional analysis of non linear electro osmotic flow with cadmium telluride nanoparticles. *Sci. Rep.* **12**, 1–16 (2022).
31. Khan, N. *et al.* Dynamics of chaotic system based on image encryption through fractal-fractional operator of non-local kernel. *AIP Adv.* **12**, 055129 (2022).
32. Murtaza, S. *et al.* Analysis and numerical simulation of fractal-fractional order non-linear couple stress nanofluid with cadmium telluride nanoparticles. *J. King Saud Univ. Sci.* <https://doi.org/10.1016/J.JKSUS.2023.102618> (2023).
33. Ahmad, Z., Bonanomi, G., di Serafino, D. & Giannino, F. Transmission dynamics and sensitivity analysis of pine wilt disease with asymptomatic carriers via fractal-fractional differential operator of Mittag-Leffler kernel. *Appl. Numer. Math.* **185**, 446–465 (2023).
34. Du, M., Wang, Z. & Hu, H. Measuring memory with the order of fractional derivative. *Sci. Rep.* **3**, 1–3 (2013).
35. Jaradat, I., Al-Dolat, M., Al-Zoubi, K. & Alquran, M. Theory and applications of a more general form for fractional power series expansion. *Chaos Solitons Fractals* **108**, 107–110 (2018).
36. Alquran, M. & Jaradat, I. A novel scheme for solving Caputo time-fractional nonlinear equations: Theory and application. *Nonlinear Dyn.* **91**, 2389–2395 (2018).
37. Murtaza, S., Kumam, P., Ahmad, Z., Seangwattana, T. & Ali, I. E. Numerical analysis of newley developed fractal-fractional model of Casson fluid with exponential memory. *Fractals* <https://doi.org/10.1142/S0218348X2240151X> (2022).
38. Wei, Z., Akgul, A., Kocamaz, U. E., Moroz, I. & Zhang, W. Control, electronic circuit application and fractional-order analysis of hidden chaotic attractors in the self-exciting homopolar disc dynamo. *Chaos Solitons Fractals* **111**, 157–168 (2018).
39. Wei, Z., Pham, V. T., Kapitaniak, T. & Wang, Z. Bifurcation analysis and circuit realization for multiple-delayed Wang-Chen system with hidden chaotic attractors. *Nonlinear Dyn.* **85**, 1635–1650 (2016).
40. Zhou, P. & Huang, K. A new 4-D non-equilibrium fractional-order chaotic system and its circuit implementation. *Commun. Nonlinear Sci. Numer. Simul.* **19**, 2005–2011 (2014).
41. Atangana, A. Fractal-fractional differentiation and integration: Connecting fractal calculus and fractional calculus to predict complex system. *Chaos Solitons Fractals* **102**, 396–406 (2017).
42. Atangana, A. & Qureshi, S. Modeling attractors of chaotic dynamical systems with fractal–fractional operators. *Chaos Solitons Fractals* **123**, 320–337 (2019).
43. Seadawy, A. R. *et al.* Modulation instability analysis and longitudinal wave propagation in an elastic cylindrical rod modelled with Pochhammer-Chree equation. *Phys. Scr.* **96**, 045202 (2021).
44. Seadawy, A. R. *et al.* Analytical mathematical approaches for the double-chain model of DNA by a novel computational technique. *Chaos Solitons Fractals* **144**, 110669 (2021).
45. Rizvi, S. T. R., Seadawy, A. R., Bibi, I. & Younis, M. Chirped and chirp-free optical solitons for Heisenberg ferromagnetic spin chains model. *Mod. Phys. Lett. B* <https://doi.org/10.1142/S021798492150139635> (2021).
46. Bilal, M. *et al.* Analytical wave structures in plasma physics modelled by Gilson-Pickering equation by two integration norms. *Results Phys.* **23**, 103959 (2021).

47. Bilal, M., Seadawy, A. R., Younis, M., Rizvi, S. T. R. & Zahed, H. Dispersive of propagation wave solutions to unidirectional shallow water wave Dullin–Gottwald–Holm system and modulation instability analysis. *Math. Methods Appl. Sci.* **44**, 4094–4104 (2021).
48. Toufik, M. & Atangana, A. New numerical approximation of fractional derivative with non-local and non-singular kernel: Application to chaotic models. *Eur. Phys. J. Plus* **132**, 1–16 (2017).
49. Qureshi, S., Atangana, A. & Shaikh, A. A. Strange chaotic attractors under fractal-fractional operators using newly proposed numerical methods. *Eur. Phys. J. Plus* **134**, 523 (2019).
50. Partohaghighi, M., Kumar, V. & Akgül, A. Comparative Study of the Fractional-Order Crime System as a Social Epidemic of the USA Scenario. *Int. J. Appl. Comput. Math.* **8**, 1–17 (2022).
51. Kapitaniak, T. *et al.* A new chaotic system with stable equilibrium: Entropy analysis, parameter estimation, and circuit design. *Entropy* **20**, 670 (2018).
52. Granas, A. & Dugundji, J. *Fixed Point Theory* <https://doi.org/10.1007/978-0-387-21593-8> (2003)
53. Ali, Z., Rabiei, F., Shah, K. & Khodadadi, T. Qualitative analysis of fractal-fractional order COVID-19 mathematical model with case study of Wuhan. *Alex. Eng. J.* **60**, 477–489 (2021).

Acknowledgements

The authors extend their appreciation to the Deanship of Scientific Research at King Khalid University for funding this work through Large Group Research Project under Grant RGP2/112/43.

Author contributions

N.K., Z.A., S.M., J.B. and H.A., conceptualized the model, N.K., S.M., J.S. and M.D.A. draw the figures, N.K., J.B., and S.W.Y. wrote the whole manuscript, Z.A., J.B., H.A. and M.D.A. supervised the project. All the authors reviewed the final draft and approved for submission.

Funding

National Natural Science Foundation of China (No. 71601072), the Fundamental Research Funds for the Universities of Henan Province (No. NSFRF210314) and Innovative Research Team of Henan Polytechnic University (No. T2022-7).

Competing interests

The authors declare no competing interests.

Additional information

Correspondence and requests for materials should be addressed to S.-W.Y.

Reprints and permissions information is available at www.nature.com/reprints.

Publisher's note Springer Nature remains neutral with regard to jurisdictional claims in published maps and institutional affiliations.



Open Access This article is licensed under a Creative Commons Attribution 4.0 International License, which permits use, sharing, adaptation, distribution and reproduction in any medium or format, as long as you give appropriate credit to the original author(s) and the source, provide a link to the Creative Commons licence, and indicate if changes were made. The images or other third party material in this article are included in the article's Creative Commons licence, unless indicated otherwise in a credit line to the material. If material is not included in the article's Creative Commons licence and your intended use is not permitted by statutory regulation or exceeds the permitted use, you will need to obtain permission directly from the copyright holder. To view a copy of this licence, visit <http://creativecommons.org/licenses/by/4.0/>.

© The Author(s) 2023